Available online at www.sciencedirect.com
ScienceDirect
Atmospheric Environment 41 (2007) 6544–6560
ATMOSPHERIC ENVIRONMENT
www.elsevier.com/locate/atmosenv

Scientific uncertainties in atmospheric mercury models II: Sensitivity analysis in the CONUS domain

Che-Jen Lin[a,b,*], Pruek Pongprueksa[a], O. Russell Bullock Jr.[c,1], Steve E. Lindberg[d,e,2], Simo O. Pehkonen[f], Carey Jang[g], Thomas Braverman[g], Thomas C. Ho[h]

[a]*Department of Civil Engineering, Lamar University, Beaumont, TX 77710, USA*
[b]*School of Environmental Science & Engineering, South China University of Technology, Guangzhou, PRC*
[c]*NOAA Air Resources Laboratory, Research Triangle Park, NC 27711, USA*
[d]*Oak Ridge National Laboratory, USA*
[e]*University of Nevada in Reno, USA*
[f]*Division of Environmental Science and Engineering, National University of Singapore, Singapore*
[g]*Office of Air Quality Planning & Standards, USEPA, Research Triangle Park, NC 27711, USA*
[h]*Department of Chemical Engineering, Lamar University, TX 77710, USA*

Received 15 January 2007; received in revised form 2 March 2007; accepted 13 April 2007

Abstract

In this study, we present the response of model results to different scientific treatments in an effort to quantify the uncertainties caused by the incomplete understanding of mercury science and by model assumptions in atmospheric mercury models. Two sets of sensitivity simulations were performed to assess the uncertainties using modified versions of CMAQ-Hg in a 36-km Continental United States domain. From Set 1 Experiments, it is found that the simulated mercury dry deposition is most sensitive to the gaseous elemental mercury (GEM) oxidation product assignment, and to the implemented dry deposition scheme for GEM and reactive gaseous mercury (RGM). The simulated wet deposition is sensitive to the aqueous Hg(II) sorption scheme, and to the GEM oxidation product assignment. The inclusion of natural mercury emission causes a small increase in GEM concentration but has little impact on deposition. From Set 2 Experiments, it is found that both dry and wet depositions are sensitive to mercury chemistry. Change in model mercury chemistry has a greater impact on simulated wet deposition than on dry deposition. The kinetic uncertainty of GEM oxidation by O_3 and mechanistic uncertainty of Hg(II) reduction by aqueous HO_2 pose the greatest impact. Using the upper-limit kinetics of GEM–O_3 reaction or eliminating aqueous Hg(II)–HO_2 reaction results in unreasonably high deposition and depletion of gaseous mercury in the domain. Removing GEM–OH reaction is not sufficient to balance the excessive mercury removal caused by eliminating the HO_2 mechanism. Field measurements of mercury dry deposition, better quantification of mercury air-surface exchange and further investigation of mercury redox chemistry are needed for reducing model uncertainties and for improving the performance of atmospheric mercury models.

Keywords: Atmospheric mercury; Chemical transport modeling; Sensitivity analysis; Model uncertainty; CMAQ-Hg

*Corresponding author. Tel.: +1 409 880 8761; fax: +1 409 880 8121.
E-mail address: Jerry.Lin@LAMAR.EDU (C.-J. Lin).
[1]In partnership with the US Environmental Protection Agency.
[2]Corporate Fellow Emeritus, now in Graeagle, CA 96103, USA.

1352-2310/$ - see front matter © 2007 Elsevier Ltd. All rights reserved.
doi:10.1016/j.atmosenv.2007.04.030

1. Introduction

Eulerian-based, first-principle atmospheric mercury models are useful tools to assess the fate of mercury in the atmosphere. The models comprehensively consider the emission, transport, chemical reactions, interfacial transfer/equilibria, cloud processes, and dry/wet deposition of mercury for process studies, source attribution and policy making. Over the years, there have been a number of such models developed to investigate the transport, chemistry and deposition of atmospheric mercury at plume (Seigneur et al., 2006a), regional (Christensen et al., 2004; Gbor et al., 2006, 2007; Lin et al., 2006a; Lin and Tao, 2003; Pai et al., 2000; Pan et al., 2006; Petersen et al., 1995, 2001; Schmolke and Petersen, 2003; Seigneur et al., 2001, 2003b; Xu et al., 2000a, b), and global scales (Bergan et al., 1999; Christensen et al., 2004; Dastoor and Larocque, 2004; Holmes et al., 2006; Seigneur et al., 2003a, 2004; Selin et al., 2007; Shia et al., 1999). These modeling studies have greatly advanced our understanding on the regional and long-range chemical transport of mercury.

One major difficulty in interpreting mercury model results arises from the uncertainties associated with the implemented model science. This is mainly caused by the incomplete understanding of mercury science that leads to different parameterizations among models. To understand the model differences, efforts in coordinated model intercomparison have been attempted. For example, the EMEP program evaluated seven atmospheric mercury models (Ryaboshapko et al., 2005). Using same inputs of mercury emission inventory (EI) and dynamic meteorology, it was found that the model-to-model variation of the simulated mercury deposition ranges from a factor of 1.5 to 6.5, with an average variation of about 2 (Bullock and Brehme, 2002; Christensen et al., 2004; Cohen et al., 2004; Petersen et al., 2001; Ryaboshapko et al., 2002, 2005 and the references cited therein). Clearly, there is a need to better understand the uncertainties leading to the observed variation.

Recently, Lin and co-workers outlined a number of model uncertainty issues in mercury emission processing, gaseous and aqueous chemistry, aqueous mercury speciation, dry and wet deposition, initial and boundary conditions (IC/BCs), domain grid resolution, and potentially missing components in the models (Lin et al., 2006b). They suggested that changes in model science processors can lead to distinct model results, and model agreement with limited field mercury measurements should not be considered as an indication of model accuracy. One approach to address model uncertainties is to perform sensitivity analyses on various model parameters, which defines the upper and lower bounds of the model outcomes caused by the uncertainties. For example, Seigneur and co-workers (Lohman et al., 2006; Seigneur et al., 2006b) studied the sensitivity of global simulations to mercury chemistry and proposed a hypothetical gaseous phase reduction of divalent mercury by sulfur dioxide to understand the chemistry uncertainty.

The objective of this study is to quantitatively assess the uncertainties of atmospheric mercury models through a series of model sensitivity experiments. This is the Part-II of the two companion papers described in Lin et al. (2006b). To contrast the work performed by Seigneur et al. (2006b) at a global scale, we carried out the simulations at a regional scale using a higher spatial resolution in a 36-km continental Unites States (CONUS) domain. The mercury model of the Community Multiscale Air Quality modeling system (CMAQ-Hg, Byun and Schere, 2006; Bullock and Brehme, 2002) was modified for this assessment. CMAQ-Hg has a large user group and is currently maintained by the Community Modeling and Analysis System (CMAS) for public release. A second objective of this study is to provide sensitivity analysis data to facilitate model improvement for the future releases of CMAQ-Hg.

2. Methods

2.1. Model domain, simulation periods and input data

The study domain covers the entire CONUS in a 36-km Lambert Conformal projection, as shown in Fig. 1. There are 148×112 horizontal grids centered at 97°W 40°N and 14 vertical layers with a surface layer thickness of about 37 m and a model top at 10,000 Pa. This is the model domain also used for the USEPA Clean Air Mercury Rule (CAMR) simulations. We selected the 2001 hourly meteorological fields for the simulations, which were also used by the USEPA for the annual simulations of criterion air pollutants. Two-monthly simulations were performed in January and July of 2001 for

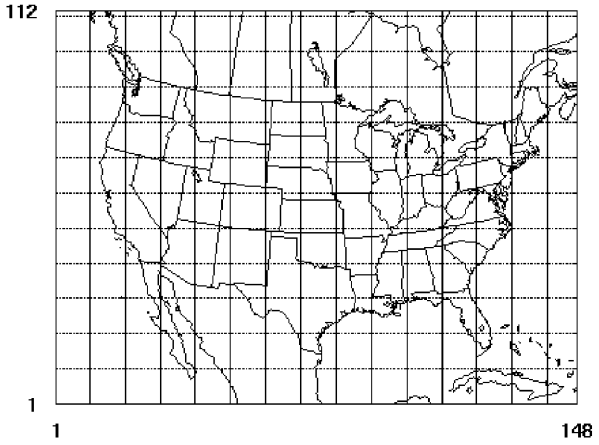

Fig. 1. The CONUS study domain in Lambert Conformal projection. The spatial resolution is 36 km with 14 vertical layers.

each sensitivity case to investigate the seasonal variation of the model results.

The meteorological data were prepared by the United State Environmental Protection Agency (USEPA) using a meso-scale meteorological model (MM5 Version 3.6, Grell et al., 1994). The raw MM5 outputs were converted into the model-ready format using a modified version of Meteorology-Chemistry Interface Processor (MCIP2, Byun and Ching, 1999) that also calculate the dry deposition velocities of gaseous elemental mercury (GEM) and reactive gaseous mercury (RGM) using the parameterization of the RADM deposition scheme in selected experiments (Lin et al., 2006b). The dry deposition velocity of particulate mercury (PHg) is assumed to be the same as that of sulfate aerosol (Bullock and Brehme, 2002).

The EI of anthropogenic mercury, criteria pollutants and other photochemical precursors was prepared using the Sparse Matrix Operator Kernel Emissions (SMOKE) Modeling System Version 2.0 by the USEPA for the CAMR simulations. The inventory of criteria pollutants and precursors was from the 1999 National Emission Inventory Estimates (NEI99) Final Version 3, and 2000 Canadian inventory. For anthropogenic mercury emission in the US, the point and area source emissions of NEI99 Hazardous Air Pollutant (HAP) inventory, with updates from municipal waste incinerators in 2002, were used. The Canadian mercury emission was based on the 2000 point and non-point emission estimates. The speciation of the anthropogenic emission followed the suggestions by Walcek et al. (2003). For selected sensitivity cases, the GEM emission from vegetation, water surfaces and soils were also included (Lin et al., 2005). Table 1 shows the anthropogenic emission of GEM, RGM and PHg entering the sensitivity simulations.

Table 1
Summary of the anthropogenic mercury emission inventory used in the sensitivity simulations

	Anthropogenic, Mg		
	January	July	Annual
GEM	5.8	5.5	66.2
RGM	2.9	2.7	32.7
PHg	0.9	0.8	9.5
Total	9.6	9.0	108.3

2.2. Chemical transport models

The chemical transport simulations were performed using the original CMAQ-Hg (Bullock and Brehme, 2002) and CMAQ-Hg version 4.5.1 (v4.5.1) released in March 2006. Version 4.5.1 is an updated version of CMAQ-Hg from the original mercury model development (Bullock and Brehme, 2002). CMAQ-Hg extensively treats the gaseous and aqueous chemical reactions, aqueous sorption of mercury onto insoluble particulates in droplets, and inter-phase transfer for GEM, RGM and PHg. In the sensitivity simulations, we modified selected science processors in CMAQ-Hg to assess the model uncertainties (more details in Section 2.3). Table 2 shows the summary of the features of CMAQ-Hg used in the simulations.

The carbon bond mechanism (CB-IV) was used as the gas-phase chemical mechanism to generate the concentrations of photochemical oxidants. The performance of the CB-IV photochemical mechanism has been demonstrated extensively. The updated gaseous mercury mechanisms (Lin and Pehkonen, 1999; Lin et al., 2006b and the references cited therein) was incorporated into the CB-IV mechanism, and the aqueous mercury chemistry is incorporated in the CMAQ's RADM cloud models. The Rosenbrock solver (ROS3 in CMAQ CCTM) was used as the chemical solver since the solver is not mechanism specific. The piecewise parabolic method (PPM) scheme was used for the advection scheme (vertical and horizontal), and the K-theory eddy diffusivity scheme was employed for the vertical diffusion.

Table 2
Summary of various versions of CMAQ-Hg used in the sensitivity simulations

Category	CMAQ-Hg (Bullock and Brehme, 2002)	CMAQ-Hg V4.5.1 (March 2006 release)	Modifications in this study
Emission inventory	Only anthropogenic emission of GEM, RGM and PHg are considered. GEM emission from natural processes (and re-emission) is assumed to be balanced by the dry deposition of GEM	Both anthropogenic and natural emissions of mercury are included	Set 1: include the natural emission by Lin et al. (2005), Case 1.2 Set 2: include both natural and re-emission input of mercury
Gas chemistry	O_3, Cl_2, H_2O_2, and OH as the oxidants. PHg as the GEM oxidation product by OH, O_3, and H_2O_2	Oxidation product by H_2O_2 changed to RGM; by OH and O_3 changed to 50% RGM and 50% PHg; kinetics of GEM oxidation by OH scaled down to 7.7×10^{-14} from $8.7\times10^{-14}\,cm^3\,molec^{-1}\,s^{-1}$	Set 1: speciate GEM oxidation products as 100% RGM, Case 1.3 Set 2: test the sensitivity of different kinetic constants, Cases 2.2–2.5 and 2.8
Aqueous chemistry	Ox: O_3, OH, HOCl, and OCl^- Red: $HgSO_3$, $Hg(OH)_2+h\nu$, HO_2	Same as Bullock and Brehme (2002)	Set 1: Same as Bullock and Brehme (2002) Set 2: test the impact of HO_2 reduction mechanism, Cases 2.6–2.7
Aqueous speciation	SO_3^{2-}, Cl^-, OH^- as the primary complexing ligands. [Cl^-] assumed to be constant	Same as Bullock and Brehme (2002)	Same as Bullock and Brehme (2002)
Aqueous sorption	Sorption of Hg(II) to ECA, bi-directional non-equilibrium kinetics with linear sorption treatment	Same as Bullock and Brehme (2002)	Set 1: test an alternative sorption scheme, Case 1.5 Set 2: Same as Bullock and Brehme (2002)
Cloud mixing scheme	RADM cloud scheme	Asymmetrical convective model (ACM) mixing scheme	Set 1: Same as Bullock and Brehme (2002) Set 2: ACM scheme (v.4.5.1).
Dry deposition	V_{dep} of HNO_3 for RGM dry deposition calculation. No GEM dry deposition considered. V_{dep} of sulfate aerosol for PHg dry deposition calculation	Both GEM and RGM deposition treated explicitly using resistance models of M3DRY scheme (Pleim et al., 1999). PHg deposition velocity treated as fine particulate in CMAQ AERO3	Both GEM and RGM (as $HgCl_2$ as in Lin et al., 2006b) deposition treated explicitly using the resistance models of RADM scheme (Wesley, 1989). PHg deposition velocity treated as fine particulate in CMAQ AERO3 (Cases 1.4 and 1.6)
Wet deposition	Scavenged PHg, dissolved and sorbed $Hg(II)_{aq}$ considered	Same as Bullock and Brehme (2002)	Set 1: Same as Bullock and Brehme (2002) Set 2: ACM scheme (v.4.5.1)

2.3. Sensitivity analysis

We performed two sets of sensitivity simulations to assess the model uncertainties. The design of the two sets of sensitivity experiments is described in Table 3. The first set of experiments was conducted to investigate the effect of the inclusion of natural emission (Lin et al., 2005), the modification of dry deposition schemes for GEM and RGM [as $HgCl_2$] (Lin et al., 2006b), the speciation of GEM oxidation products, the aqueous adsorption, and the combination of above scientific processors. To show the difference between the original CMAQ-Hg and v4.5.1, the model results using identical EI and meteorological data was also compared. In Set 1 Experiments, the model results of the original CMAQ-Hg (Bullock and Brehme, 2002) were used as the base case for comparison. A prescribed set of IC/BCs for GEM, RGM and PHg was obtained from interpolating the elevation-dependent concentration shown in Table 4.

The second set of experiments focus on the kinetic uncertainty of mercury chemistry in both gaseous

Table 3
The two sets of sensitivity simulations performed in this study (detailed model settings listed in Table 2)

Set 1 Experiments: alternative model implementations		Set 2 Experiments: chemical kinetic uncertainty	
Case no.	Descriptions	Case no.	Descriptions
1.1	CMAQ-Hg as in Bullock and Brehme (2002)	2.1	CMAQ-Hg Version 4.5.1 (released March 2006)
1.2	Include natural emission of GEM in Hg EI as in Lin et al. (2005)	2.2	Zero-out gaseous oxidation of GEM by OH
1.3	Speciate mercury oxidation products to 100% RGM (Seigneur et al., 2001)	2.3	Zero-out gaseous oxidation of GEM O_3
1.4	Incorporate the dry deposition schemes for GEM and RGM (as $HgCl_2$) as in Lin et al. (2006b)	2.4	Zero-out gaseous oxidation of GEM by both OH and O_3
1.5	Treat aqueous Hg(II) sorption as a Langmuir sorption isotherm as in Lin et al. (2006b)	2.5	Use the upper kinetic limit for GEM–O_3 reaction (Pal and Ariya, 2004; 7.5×10^{-19} cm^3 $molec^{-1}$ s^{-1})
1.6	Combine the modifications of Cases 1.2–1.5	2.6	Zero-out aqueous reduction of Hg(II) by HO_2
1.7	CMAQ-Hg version 4.5.1 using identical mercury EI (from anthropogenic sources only) and meteorology as Case 1.1[a]	2.7	Zero-out both aqueous reduction of Hg(II) by HO_2 and gaseous oxidation of GEM by OH
		2.8	Speciate mercury oxidation products to 100% RGM (Seigneur et al., 2001)

[a]In Case 1.7, the kinetics of GEM oxidation by OH was not scaled down to 7.7×10^{-14} from 8.7×10^{-14} cm^3 $molec^{-1}$ s^{-1} as in v4.5.1 for consistency in kinetic constants compared to all other Set 1 cases. The difference between Case 1.6 and 1.7 is in the dry deposition schemes and the speciation of GEM oxidation products. Case 1.6 uses RADM scheme and speciates the GEM oxidation products as 100% RGM; while Case 1.7 uses M3DRY scheme for estimating the dry deposition velocity of GEM and RGM, and speciates the oxidation products as 50% RGM and 50% PHg.

Table 4
Mercury concentration used as the initial and boundary conditions

Sigma (σ) level (layer top, m AMSL)	0.98 (146)	0.93 (521)	0.84 (1,234)	0.60 (3,447)	0.30 (7,281)	0.00 (14,657)
GEM (ppmv)[a]	1.78×10^{-07}	1.77×10^{-07}	1.76×10^{-07}	1.75×10^{-07}	1.74×10^{-07}	1.73×10^{-07}
RGM (ppmv)[a]	2.00×10^{-09}	3.00×10^{-09}	4.00×10^{-09}	5.00×10^{-09}	6.00×10^{-09}	7.00×10^{-09}
PHG (pg m^{-3})	19.4	19.0	17.8	14.0	9.0	3.0

[a]ppmv $\times$ 40,893 $\times$ M.W. = ng m^{-3} @ 1 atm and 25 °C.

and aqueous phases, particularly the GEM oxidation by O_3 and OH and the $Hg(II)_{(aq)}$ reduction by HO_2 as suggested in recently published literatures (Calvert and Lindberg, 2005; Gardfeldt and Jonsson, 2003; Lin et al., 2006b; Pal and Ariya, 2004a, b; Pehkonen and Lin, 1998). For gaseous mercury redox chemistry, the sensitivity experiments were designed to investigate the effect of a range of GEM oxidation kinetics and the oxidation product distribution on the simulated mercury deposition. For aqueous mercury redox chemistry, the sensitivity of model results to the controversial Hg(II) reduction by HO_2 was tested. In Set 2 Experiments, the model output of CMAQ-Hg v4.5.1 was used as the base case for comparison.

The model performance of each sensitivity case was evaluated against the monthly wet deposition data archived by the mercury deposition network (MDN). Since the same deposition flux can be obtained by different combinations of precipitation and aqueous concentration, we selected the model grids where the measured and modeled precipitation data are within $\pm 50\%$ of agreement for model verification to avoid the compensation errors of precipitation and concentration. Using the 50% precipitation disagreement as data screening criteria is a balance between maintaining sufficient number of data points for model verification and eliminating the bias from model meteorology. Through this QA/QC routine, the model performance decreased slightly. However, we feel that it is important to screen out the data points that give good model results for wrong scientific reasons to better evaluate model uncertainties.

3. Results and discussion

3.1. Set 1 Experiments

3.1.1. Base case results (Case 1.1)

Fig. 2 shows the July 2001 simulation results of the monthly average concentration (GEM + RGM + PHg), and the accumulated monthly dry and wet deposition from Set 1 Experiments. The January cases exhibit similar trends and only the comparison to MDN data are shown (Fig. 3a and 4a). From the base case results, it is clear that elevated mercury concentration occurs only at the locations near large anthropogenic emission sources (e.g., Northeast US and West Coast, Fig. 2a.1). The modeled total mercury concentration is dominated by GEM (>98% throughout the domain). The dry deposition is mainly contributed by RGM deposition (>99%), due to the high surrogate dry deposition velocity (V_{dep,HNO_3}) and no GEM deposition implemented in the original CMAQ-Hg (Bullock and Brehme, 2002; Lindberg and Stratton, 1998). From Figs. 2b.1 and 2c.1, the dry deposition intensity is much weaker than the wet deposition because the original CMAQ-Hg speciates the GEM oxidation products as 100% PHg (i.e., no RGM is produced from the chemistry). The model wet deposition flux is contributed comparably by the dissolved Hg(II) and scavenged PHg in the droplets. The dissolved Hg(II) speciation is dominated by $HgCl_2$ with the calculated aqueous Cl^- concentration ($\sim$10 μM). The regions with high wet deposition of mercury coincide with the grids with high precipitation.

3.1.2. Effect of including natural emission (Case 1.2)

By incorporating the GEM emission from natural sources (ca. 9 Mg in July 2001, Lin et al., 2005), a small increase of 0.05–0.2 ng m^{-3} of GEM concentration is observed (Figs. 2a.1 and 2a.2). Such an increase is somewhat smaller compared to the results by Gbor et al. (2006) that reported an average increase of 0.2 ng m^{-3} in GEM concentration. This is caused by their higher natural mercury emission estimate (about 3 times greater for the same aerial coverage). For the January simulation, the increase in mercury concentration is negligible due to the much weaker natural emission in winter months (Lindberg et al., 2002). From Figs. 2b.2 and 2c.2, adding natural GEM emission to the EI input has little impact on the simulated dry and wet deposition, since the small increase in GEM concentration does not significantly enhance the production of RGM and PHg.

3.1.3. Effect of GEM oxidation product speciation (Case 1.3)

The original CMAQ-Hg treats all the GEM oxidation products by OH, O_3, and H_2O_2 as PHg, presumably as HgO, due to its low vapor pressure (Schroeder and Munthe, 1998). Some other models consider the oxidation products remain in the gaseous phase as RGM (Pai et al., 1997, 1999; Seigneur et al., 2004). In Case 1.3, treating the GEM oxidation products as RGM (as compared to PHg) enhances the dry removal of mercury (Fig. 2b.3), particularly in the regions with high photochemical activities. This leads to a lower total mercury concentration (Fig. 2a.3). The intensity of simulated wet deposition also reduces significantly (Fig. 2c.3). This is mainly caused by the low PHg concentration since anthropogenic emission and IC/BCs of PHg are the only source in the absence of chemical production of PHg in the sensitivity case. More quantitative discussion for a similar case is given in Section 3.2 with the data obtained from the Set 2 Experiments.

3.1.4. Effect of incorporating GEM and RGM dry deposition schemes (Case 1.4)

Figs. 2a.4, 2b.4 and 2c.4 show the effect of incorporating a dry deposition scheme that calculates the deposition velocity (V_{dep}) of GEM and RGM (treated as $HgCl_2$) using the RADM resistance model (Lin et al., 2006b). Compared to the base case where GEM deposition is not considered and V_{dep,HNO_3} is used as a surrogate $V_{dep,RGM}$, the calculated $V_{dep,RGM}$ in Case 1.4 is about 50% smaller (Lin et al., 2006b). However, combining the dry deposition of GEM and RGM, more mercury is removed from the gaseous phase (Fig. 2a.4), and the dry deposition increases significantly (Fig. 2b.4) compared to the base case. Of the total dry deposition, nearly two-thirds is contributed by GEM deposition and slightly more than one-third is contributed by RGM deposition. The increased dry deposition occurs mainly in the continent due to the greater deposition velocity over land surfaces and vegetation compared to over water surfaces (Lindberg et al., 1992). On the other hand, the incorporation of dry deposition processes does not significantly affect the simulated wet deposition fluxes (Fig. 2c.4), since

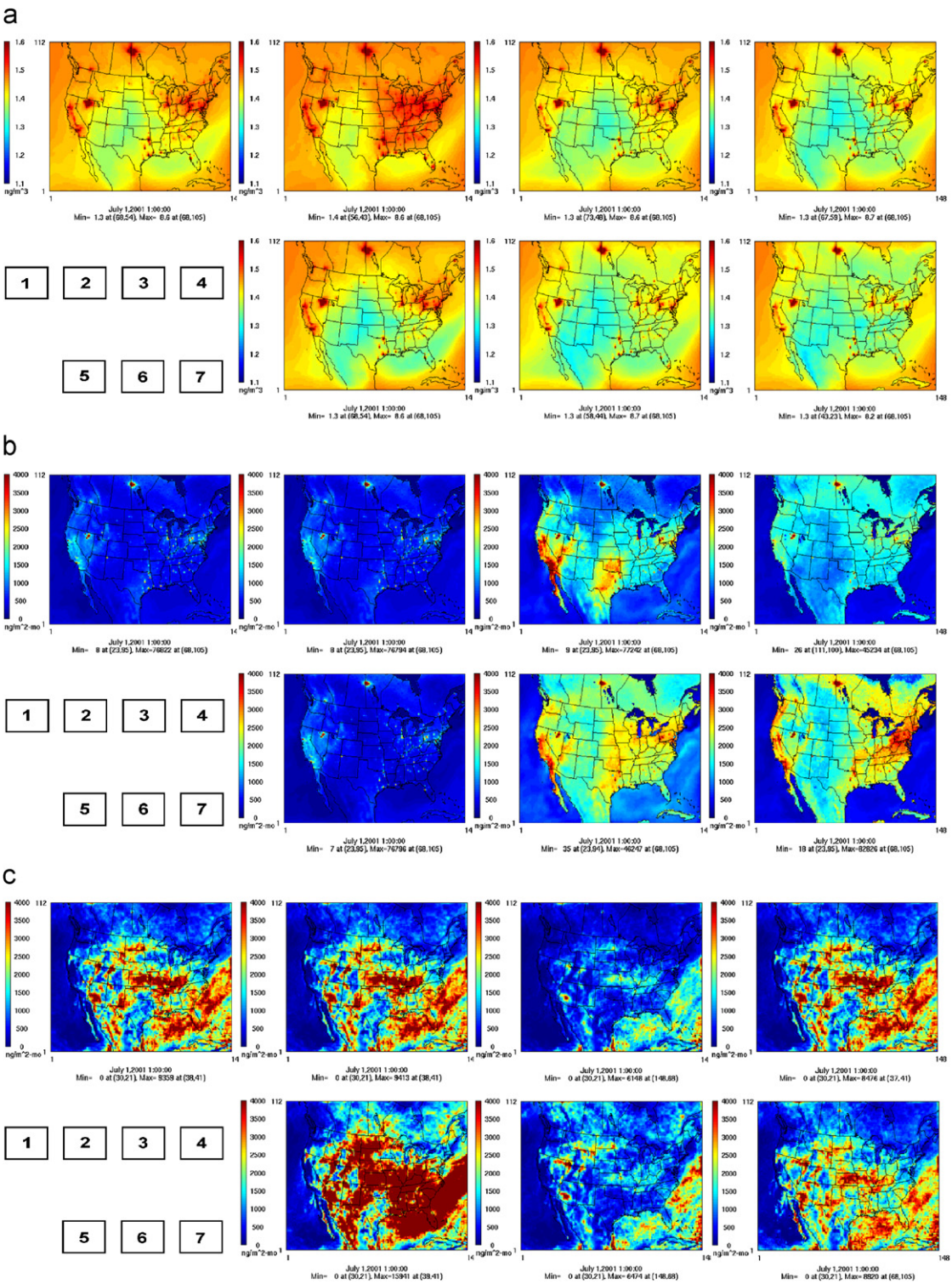

Fig. 2. Simulation results of Set 1 Experiments: (a) monthly average total mercury concentration, (b) accumulated monthly dry deposition, and (c) accumulated monthly wet deposition. The Set 1 case numbers are indicated in each subplot.

the chemistry and cloud process remains the same as the base case.

3.1.5. Effect of incorporating sorption equilibrium for aqueous sorption scheme (Case 1.5)

Case 1.5 tested an alternative aqueous adsorption scheme for dissolved $Hg(II)_{(aq)}$. In the original CMAQ-Hg (Case 1.1), the sorption algorithms have equal adsorption and desorption rate. As a result, the adsorption is insensitive to the implemented sorption constant and soot concentration in droplets, which is inconsistent with experimental observations (Seigneur et al., 1998). The tested sorption scheme uses a reduced form of Langmuir isotherm at dilute substrate concentration as described in Lin et al. (2006b). The implemented sorption constant is based on the experimental work by Sanchez-Polo and Rivera-Utrilla (2002) as compared to Seigneur et al. (1998) in the original CMAQ-Hg. With the alternative sorption treatment, a greater fraction of aqueous Hg(II) is drawn to the particulate phase in droplets, causing a significantly greater wet deposition (Fig. 2c.5) and more mercury removal from the gaseous phase (Fig. 2a.5). This modification has a negligible effect on the dry deposition (Fig. 2b.5).

3.1.6. Combined effect of Cases 1.2–1.5 modifications and comparison to CMAQ-Hg v4.5.1 (Cases 1.6 and 1.7)

Combining the model science modifications of Cases 1.2–1.5 removes mercury from the gaseous phase more rapidly through the dry deposition of GEM and RGM (Fig. 2a.6). This is due to the inclusion of GEM dry deposition and the production of RGM from the gaseous oxidation of GEM (Fig. 2b.6). The wet deposition is slightly lower compared to the base case, a result of the combined effect of Cases 1.3 and 1.5. Compared Case 1.6 results to the simulation results by CMAQ-Hg v4.5.1 (the model difference is shown in Tables 2 and 3), v4.5.1 produces a greater dry deposition (Fig. 2b.7) due to the slightly higher $V_{dep,GEM}$ and $V_{dep,RGM}$ calculated from M3DRY deposition scheme compared to the RADM scheme, and a greater wet deposition because the 50% PHg produced from GEM oxidation is scavenged into the aqueous phase (Fig. 2c.7).

3.1.7. Comparisons between model results and MDN data

The model results from Cases 1.1 to 1.7 were compared to the observed aqueous concentration (Fig. 3) and wet deposition (Fig. 4) of mercury at the respective MDN sites. The model performance statistics (slope and R^2) is shown in Table 5. The model and measurement precipitation have good agreement (slope = 0.846, $R^2 = 0.892$ for January, slope = 1.069, $R^2 = 0.871$ for July). The original CMAQ-Hg (Case 1.1) slightly over-estimates the concentration and deposition in both months. Including natural emission does not change the simulated wet deposition results compared to the base case (Case 1.2). Speciating GEM oxidation products as RGM (as compared to PHg in the base case) decreases the PHg scavenged into the aqueous phase, and leads to a lower wet deposition intensity (Case 1.3). Changing the dry deposition scheme mainly influences the dry deposition flux and has little effect on wet deposition (Case 1.4). Incorporating the sorption scheme significantly partitions aqueous mercury to the particulate phase, resulting in greater wet deposition (Case 1.5). Combining all the Set 1 modifications (Case 1.6) yields slightly better overall model performance (slope closer to 1) compared to other cases in the Set 1 Experiments, particularly in July 2001.

3.2. Set 2 Experiments

From the Set 1 Experiments, it appears that mercury chemistry and aqueous sorption have the greatest impact on the simulated wet deposition; and the chosen dry deposition scheme has the greatest impact on the simulated dry deposition flux. In the Set 2 Experiments (Table 3), we focused on the response of simulated wet deposition to mercury chemistry. In this set of simulations, the "re-emission" of mercury (Seigneur et al., 2004) was also included in the simulations to compensate for the dry deposition of mercury estimated by the M3DRY deposition scheme in CMAQ-Hg v4.5.1. Other simulation results are summarized as bar charts for inter-case comparison.

3.2.1. Impact of mercury chemistry on modeled wet deposition

Fig. 5 shows the effect of mercury chemistry uncertainty on the simulated total mercury wet deposition for July 2001. The January 2001 results show similar trends and only model performance statistics are shown. The model performance statistics for both months are shown in Table 5. Fig. 5.1 illustrates the simulated mercury deposition using the default model settings of CMAQ-Hg

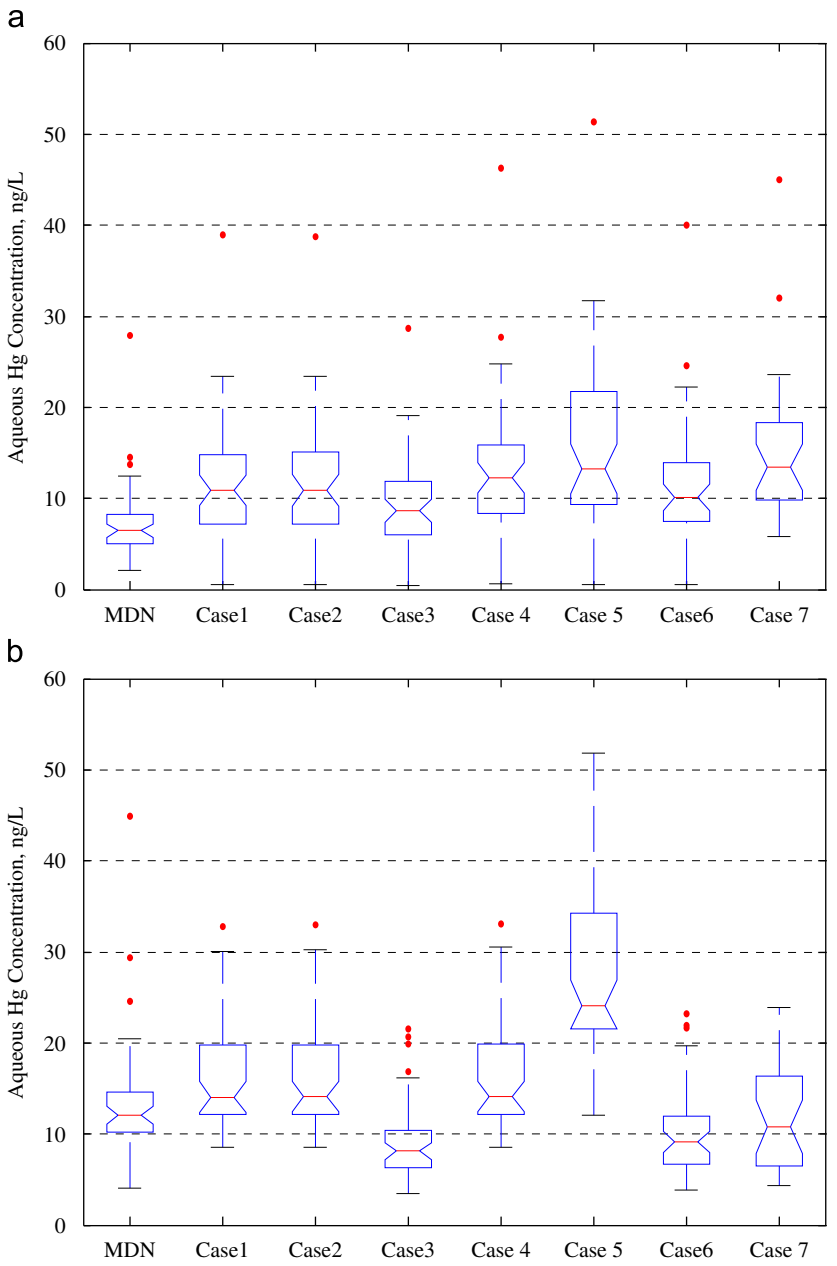

Fig. 3. Comparison of modeled concentrations of total aqueous mercury for Set 1 Experiments: (a) January 2001, and (b) July 2001.

v4.5.1, which underestimates the observed wet deposition (slope = 0.66). The wet deposition flux is slightly smaller than Fig. 2c.7 since the default settings of CMAQ-Hg v4.5.1 scales down the GEM oxidation rate by OH by 12% (Table 3). Figs. 5.2–5.4 show the role of OH and O_3 chemistry in mercury wet deposition. Removing the OH oxidation mechanism results in a much weaker wet deposition (Fig. 5.2, slope = 0.37) compared to removing the O_3 oxidation mechanism (Fig. 5.3, slope = 0.64), indicating OH is a more dominating oxidant of GEM in the model. Removing both GEM oxidation reactions provides an indication of the wet deposition directly contributed from anthropogenic emission, since there is no other important oxidant removing GEM (Fig. 5.4).

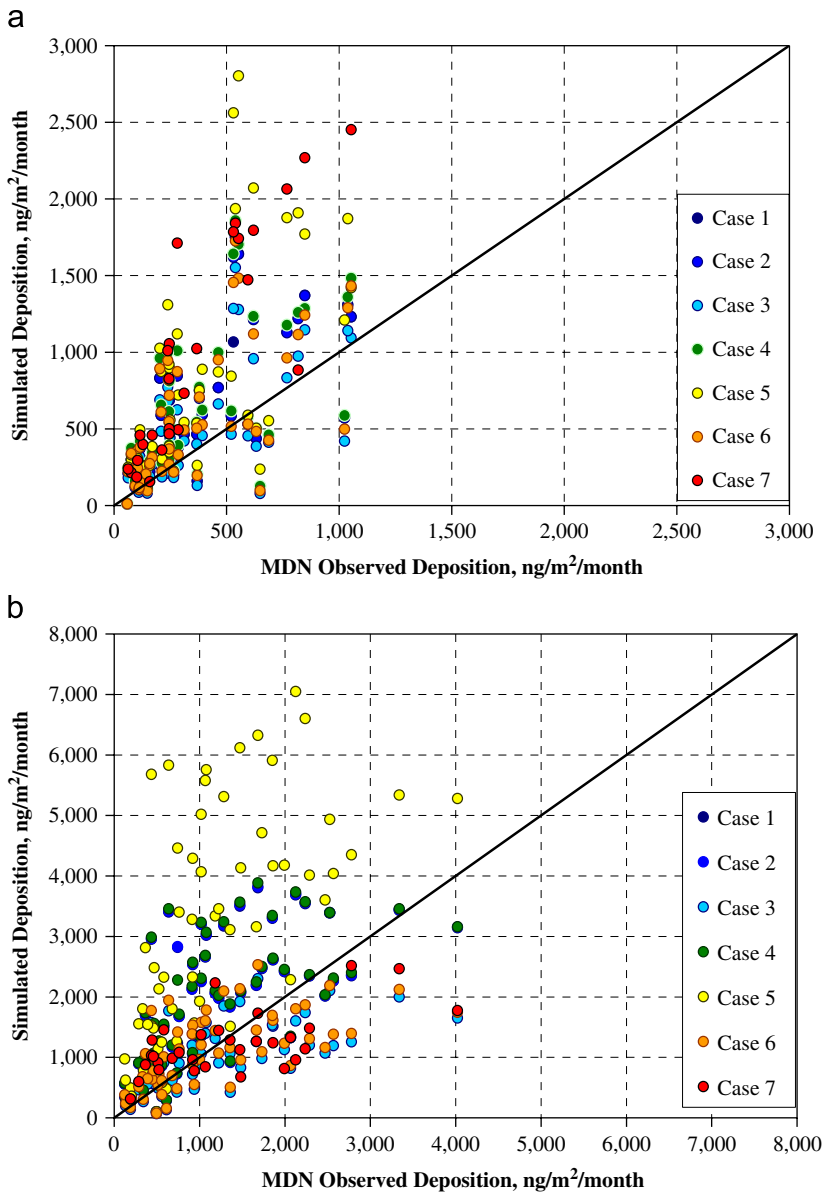

Fig. 4. Comparison of simulated mercury wet deposition to MDN-observed wet deposition for Set 1 Experiments: (a) January 2001, and (b) July 2001.

Implementing the recently reported rate constant (Pal and Ariya, 2004b) for GEM-O_3 reaction causes much greater wet deposition through the scavenging of both PHg and RGM (Fig. 5.5). With the much lager rate constant, O_3 becomes the most dominant oxidant of GEM in model chemistry (slope = 1.22), and the reaction rate should be considered as an upper limit (Seigneur et al., 2006b), since the oxidation may also be contributed by other heterogeneous processes (Calvert and Lindberg, 2005).

Removing the controversial aqueous Hg(II) reduction by HO_2 (Gardfeldt and Jonsson, 2003) results in unreasonably high wet deposition (Fig. 5.6, slope = 2.69), and also causes rapid mercury depletion in the gaseous phase. This is due to a lack of reduction mechanism in the model. The other reduction reactions of aqueous Hg(II) are mediated by dissolved S(IV) and $Hg(OH)_2$ photolysis. However, the lifetime of dissolved S(IV) is relatively short (a few hours) and its aqueous

speciation with Hg(II) is typically dominated by the non-reactive $Hg(SO_3)_2$. The rate of $Hg(OH)_2$ photoreduction is negligible. Under such conditions, HO_2 is the only important reductant to balance the oxidation of elemental mercury in the model (Lin and Pehkonen, 1998, 1999). Since the occurrence of GEM oxidation by OH has also been questioned (Calvert and Lindberg, 2005), Case 2.7 tests if simultaneously removing the GEM oxidation by OH and aqueous Hg(II) reduction by HO_2 would produce a more reasonable wet deposition pattern. As shown in Fig. 5.7, eliminating GEM oxidation by OH is not sufficient to balance the reduction of Hg(II) by HO_2. This is different from the model results using a global model by Seigneur et al. (2006b), which reported that the reduction of Hg(II) by HO_2 (or a reaction with a similar overall rate) is needed to balance the oxidation of GEM by OH and O_3, but is not needed if the gas-phase oxidation of GEM by OH is eliminated. Changing the GEM oxidation products from 50/50 RGM/PHg to 100% RGM slightly reduces wet deposition (Case 2.8). This is because model chemistry does not produce PHg, and the produced RGM is rapidly removed through dry deposition. As a result, less mercury is wet scavenged and removed compared to the base case (Fig. 5.8). The simulated wet deposition overestimates the MDN observations in the January cases (Table 5), indicating that there may be systematic model bias for winter simulations using CMAQ v.4.5.1.

Table 5
Model performance statistics for the sensitivity experiments[a]

Case number	Set 1 Experiments				Set 2 Experiments			
	January		July		January		July	
	Slope	R^2	Slope	R^2	Slope	R^2	Slope	R^2
1	1.37	0.77	1.32	0.79	1.88	0.81	0.66	0.76
2	1.40	0.76	1.32	0.79	1.79	0.80	0.37	0.61
3	1.16	0.76	0.70	0.79	1.81	0.81	0.64	0.76
4	1.50	0.76	1.33	0.79	1.69	0.80	0.34	0.59
5	1.99	0.75	2.27	0.78	3.15	0.83	1.22	0.78
6	1.36	0.76	0.77	0.78	4.15	0.82	2.69	0.74
7	2.56	0.91	0.72	0.81	3.88	0.82	1.99	0.66
8	n/a	n/a	n/a	n/a	1.82	0.81	0.49	0.70

[a]Model results overestimate measurements when slope is greater than 1.0.

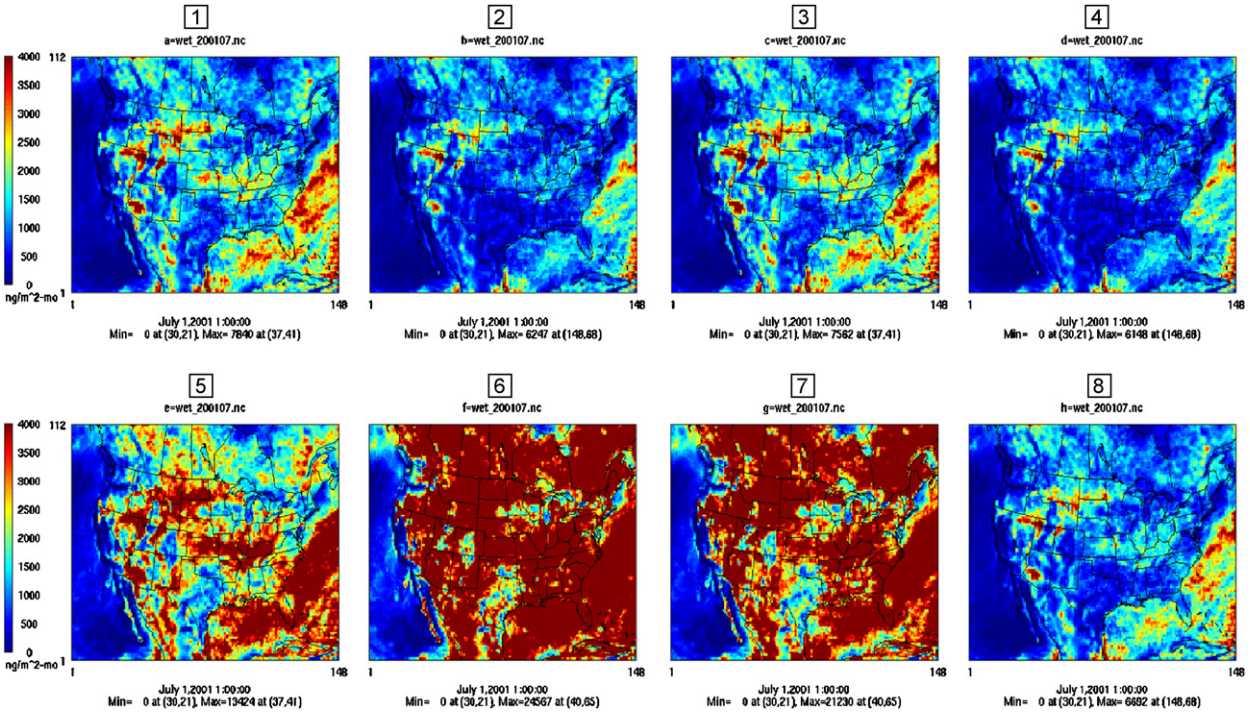

Fig. 5. Effect of mercury chemistry treatment (Set 2 Experiments) on the simulated total mercury wet deposition in the domain. The number above each subplot indicates its respective case number in Set 2 Experiments.

3.2.2. Sensitivity of simulated dry and wet deposition to model chemistry

Fig. 6 compares the speciated mercury deposition from Set 2 Experiments. The total dry deposition is dominated by RGM, although GEM also contributes significantly (Fig. 6a). Compared to Case 1.3 (Section 3.1.4), the contribution from RGM is much greater in Set 2 Experiments because the GEM oxidation product is assigned to 100% PHg in Case 1.3. PHg deposition is not important in mercury dry deposition, because its particles size is in the fine mode. This leads to a very small deposition velocity and deposition flux (Lin et al., 2006b). Since the employed dry deposition scheme is identical for the sensitivity cases (M3DRY), the difference in the simulated dry deposition from Set 2 Experiments is quite moderate except in Cases 2.5 and 2.6. This indicates that the current mechanistic and kinetic uncertainties associated with the GEM oxidation by O_3 and the aqueous phase reduction of Hg(II) pose the greatest potential for model bias in dry deposition. This also implies that aqueous chemistry (e.g., Hg(II) reduction by HO_2) of mercury is sufficiently strong to affect the simulated dry deposition.

From Fig. 6b, it is clear that the total wet deposition is dominated by RGM, although PHg

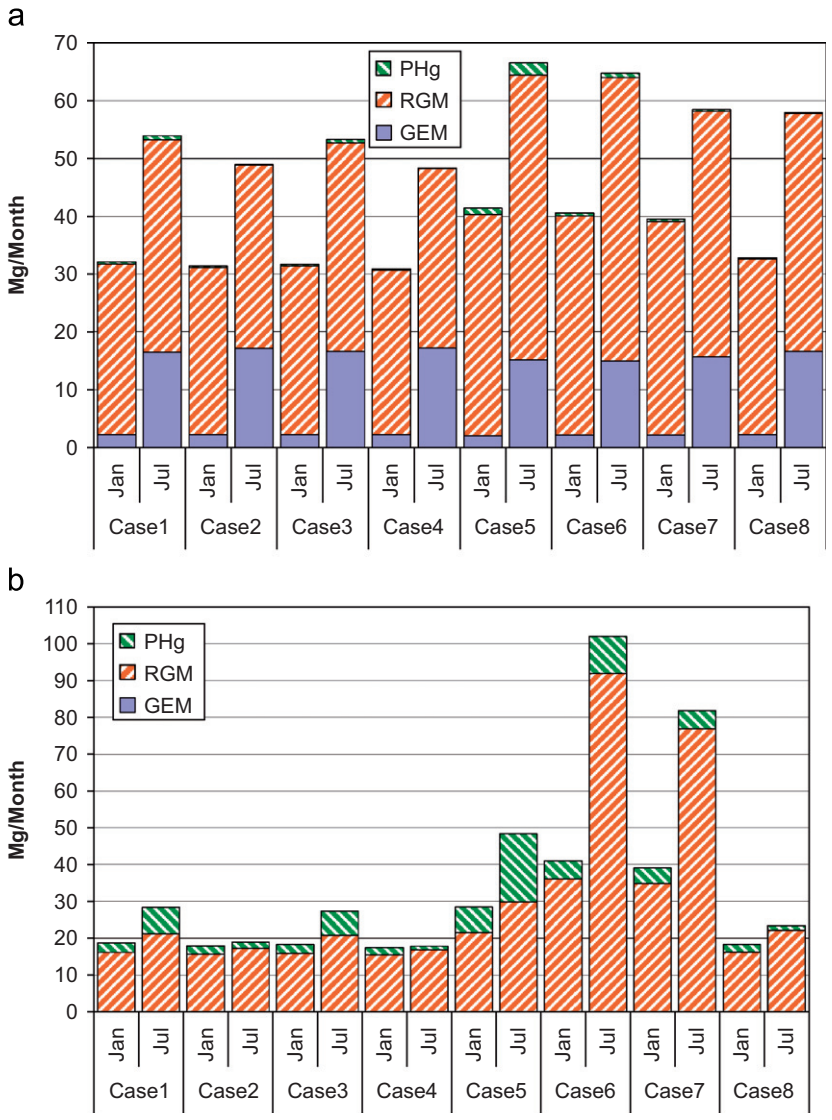

Fig. 6. Comparison of simulated *speciated* mercury deposition in the domain for Set 2 Experiments: (a) dry deposition, and (b) wet deposition.

can contribute considerably in the summer (Fig. 6b). There is little wet deposition of GEM because of the low solubility of GEM in water. The GEM oxidation by O_3 and the aqueous Hg(II) reduction by HO_2 have the greatest impact on the simulated wet deposition (Cases 2.6 and 2.7). In Case 2.8, although the change in the oxidation product speciation affects somewhat the dry and wet deposition intensity and its contributing species (Figs. 6a and 6b), the sum of dry and wet deposition does not change compared to the base case (Case 2.1).

3.2.3. *Sensitivity of total deposition contribution to chemistry treatment*

One question that is often asked in the atmospheric cycling of mercury is the relative importance of dry and wet deposition, and the relative contribution from different mercury species being removed from the atmosphere. With the model results from Set 2 Experiments, these relative contributions are compared. From Fig. 7a, it can be seen that the most important deposited species is RGM, accounting for at least 65% (average 80%) of the total (dry and wet) deposition among all the

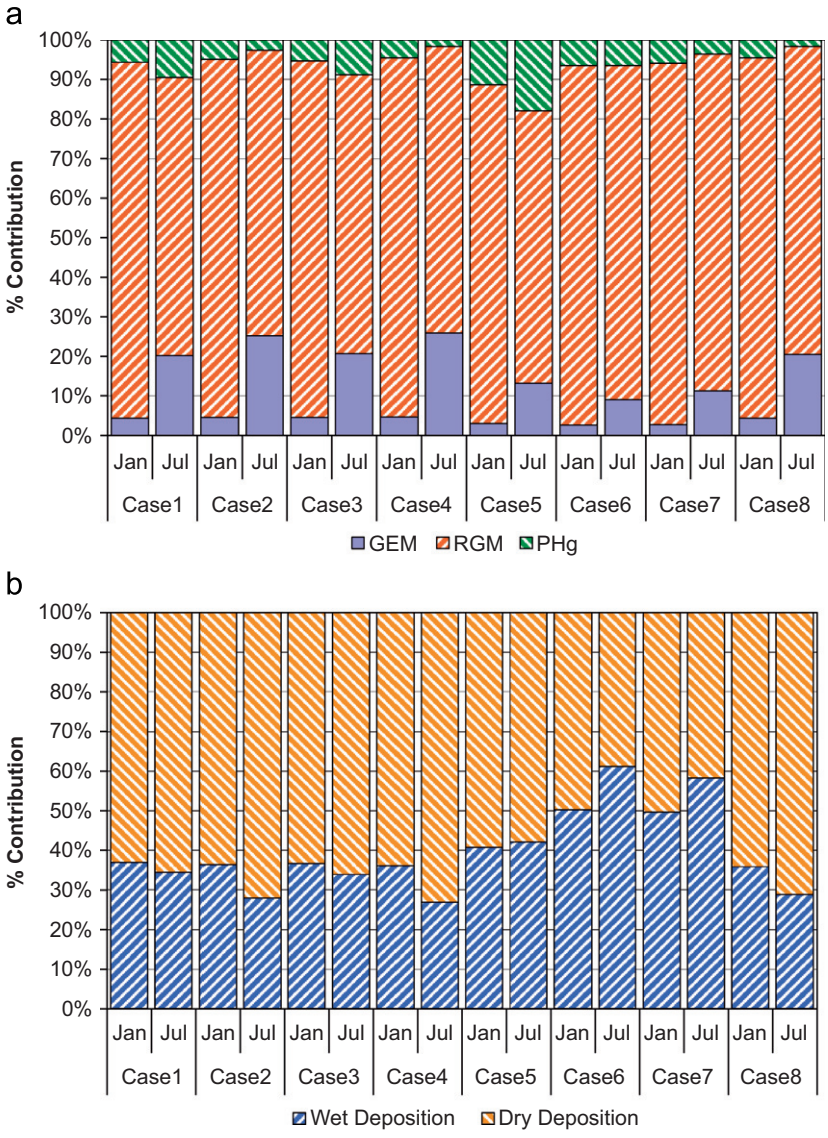

Fig. 7. Comparison of simulated *total* mercury deposition in the domain for Set 2 Experiments: (a) contribution from different mercury species, and (b) contribution from wet and dry deposition. Note that in (a) the adsorbed Hg(II) in the aqueous phase is considered as PHg.

sensitivity cases. The next important species is GEM, mainly removed through dry deposition, contributing to an average of 20% of total deposition in the summer month. However, its contribution in January is much smaller (5%) due to the lack of lush vegetation and its dry deposition velocity in the cold month. It should also be noted that net GEM deposition in all sensitivity cases has little variation. PHg constitutes 2–18% of the total mercury removal among the cases, mainly through wet processes.

From Fig. 7b, it can be seen that the default model settings of CMAQ-Hg v4.5.1 estimates that about 35% of the total mercury deposition is through wet processes, and about 65% is through dry processes. Interestingly, the relative contribution does not have much variation in January and July for the base case (Case 2.1). However, modifying the mercury chemical mechanism has a considerable impact on the relative contribution, with the wet deposition contribution ranging from 27% to 61% among the cases. The greatest impact comes from eliminating the HO_2 reduction mechanism (Case 2.6), which forces the oxidized mercury to stay oxidized and contained in the aqueous phase. This gives a very strong wet removal and causes the depletion of GEM. Nevertheless, the dry and wet deposition has comparable contribution in all cases; with the dry removal dominating over the wet removal up to 2:1 ratio.

4. Implications and conclusions

In this study, we performed a series of sensitivity simulations to quantitatively assess the scientific uncertainties of atmospheric mercury models using modified versions of CMAQ-Hg in a 36-km CONUS domain. The sensitivity cases cover a wide range of model treatments, including gas phase chemistry, aqueous phase chemistry, aqueous phase adsorption, dry deposition, and EI processing. The model results indicate that the simulated mercury dry deposition is sensitive to the GEM oxidation product assignment, and to the implemented dry deposition scheme for GEM and RGM. The simulated wet deposition is sensitive to the aqueous Hg(II) sorption scheme, and the GEM oxidation product assignment. The inclusion of natural emission causes a small increase of GEM concentration but have little impact on deposition. Under the default model configurations of CMAQ-Hg, OH is the most important oxidant responsible for removing atmospheric mercury. However, O_3 becomes the dominant oxidants if the upper-limit kinetics of the GEM–O_3 reaction is implemented in the model. Simulated dry deposition accounts for up to two-thirds of total mercury removal from the atmosphere, and the total deposited mercury is mainly contributed by RGM for both dry and wet removal processes.

Model treatment of mercury chemistry has a greater impact on simulated wet deposition than on dry deposition. Among the known mercury reactions, the kinetic uncertainty of GEM oxidation by O_3 and the mechanistic uncertainty of Hg(II) reduction by aqueous HO_2 have the greatest impact on simulated mercury deposition. Using the upper-limit kinetics of GEM–O_3 reaction or eliminating Hg(II)–HO_2 reaction causes unreasonably high deposition and rapid depletion of gaseous mercury. Removing GEM–OH reaction from mercury chemistry is not sufficient to balance the deposition (especially for wet deposition) and GEM depletion caused by eliminating the HO_2 mechanism. Therefore, if the reduction of aqueous Hg(II) by HO_2 did not occur in atmospheric droplets as suggested by Gardfeldt and Jonsson (2003), there should be some other divalent mercury reduction mechanism with a similar overall rate to balance the oxidation rate of elemental mercury for the model to perform consistently with our understanding of atmospheric mercury processes. Recently, there are modeling efforts that implement alternative gaseous reduction mechanisms of divalent mercury by SO_2 (Lohman et al., 2006; Seigneur et al., 2006b), CO and photoreduction of RGM (Pongprueksa et al., 2006). Although these model results agree reasonably well with field measurements, these mechanisms need to be carefully verified with laboratory investigations to confirm their significance in atmospheric mercury chemistry for future model improvement.

Another model uncertainty area that requires more research attention is the treatment of air-surface exchange of mercury. Recently, modeling efforts have been attempted to estimate the evasion flux using semi-mechanistic or regression models from vegetative, soil and water surfaces (e.g., Bash et al., 2004; Gbor et al., 2006; Lin et al., 2005; Xu et al., 1999). These modeling approaches consider vegetation as strong mercury emission sources, and soils and water as weak emission sources based on earlier flux measurements. However, more recent measurements made by Gustin and co-workers

under controlled experimental conditions (Ericksen and Gustin, 2004, 2006; Gustin et al., 2006; Obrist et al., 2005) suggested that soil emission is perhaps a stronger source, and that vegetation may be a net sink for mercury. More research is clearly needed to better understanding these processes for model formulation and implementation.

More field data of mercury deposition are critical to providing more constrains for model science implementation. Measurement of speciated dry deposition flux will be very useful for verifying the dry mercury removal processes in the models. Furthermore, since oxidation of GEM is an important driving force for the simulated concentration and deposition, observational networks for GEM and RGM will also be needed for model verification and for constructing more realistic initial and boundary conditions.

Acknowledgments

The authors would like to acknowledge the funding support from Texas Commission on Environmental Quality (TCEQ Work Order Number: 64582-06-15) and the USEPA Office of Air Quality Planning & Standards (RTI Subcontract Number: 6-321-0210288) for this work. A portion of the research presented here was performed under the Memorandum of Understanding between the U.S. Environmental Protection Agency (EPA) and the U.S. Department of Commerce's National Oceanic and Atmospheric Administration (NOAA) and under agreement number DW13921548. This work constitutes a contribution to the NOAA Air Quality Program. Although it has been reviewed by EPA and NOAA and approved for publication, it does not necessarily reflect their policies or views.

References

Bash, J.O., Miller, D.R., Meyer, T.H., Bresnahan, P.A., 2004. Northeast United States and Southeast Canada natural mercury emissions estimated with a surface emission model. Atmospheric Environment 38 (33), 5683–5692.

Bergan, T., Gallardo, L., Rodhe, H., 1999. Mercury in the global troposphere: a three-dimensional model study. Atmospheric Environment 33 (10), 1575–1585.

Bullock, O.R., Brehme, K.A., 2002. Atmospheric mercury simulation using the CMAQ model: formulation description and analysis of wet deposition results. Atmospheric Environment 36 (13), 2135–2146.

Byun, D.W., Ching, J.K.S., 1999. Science algorithms of the EPA models-3 Community Multiscale Air Quality (CMAQ) modeling system. Rep EPA-600/R-99/030. Office of Research and Development, US Environmental Protection Agency, Washington, DC.

Byun, D.W., Schere, K.L., 2006. Review of the governing equations, computational algorithms, and other components of the models-3 Community Multiscale Air Quality (CMAQ) modeling system. Applied Mechanics Review 59, 51–77.

Calvert, J.G., Lindberg, S.E., 2005. Mechanisms of mercury removal by O-3 and OH in the atmosphere. Atmospheric Environment 39 (18), 3355–3367.

Christensen, J.H., Brandt, J., Frohn, L.M., Skov, H., 2004. Modelling of mercury in the Arctic with the Danish Eulerian hemispheric model. Atmospheric Chemistry and Physics 4, 2251–2257.

Cohen, M., et al., 2004. Modeling the atmospheric transport and deposition of mercury to the Great Lakes. Environmental Research 95 (3), 247–265.

Dastoor, A.P., Larocque, Y., 2004. Global circulation of atmospheric mercury: a modelling study. Atmospheric Environment 38 (1), 147–161.

Ericksen, J.A., Gustin, M.S., 2004. Foliar exchange of mercury as a function of soil and air mercury concentrations. Science of the Total Environment 324 (1–3), 271–279.

Ericksen, J., Gustin, M.S., 2006. Air-surface exchange of mercury with soils amended with ash materials. Journal of the Air & Waste Management Association 56 (7), 977–992.

Gardfeldt, K., Jonsson, M., 2003. Is bimolecular reduction of Hg(II) complexes possible in aqueous systems of environmental importance. Journal of Physical Chemistry A 107 (22), 4478–4482.

Gbor, P.K., et al., 2006. Improved model for mercury emission, transport and deposition. Atmospheric Environment 40 (5), 973–983.

Gbor, P.K., et al., 2007. Modeling of mercury emission, transport and deposition in North America. Atmospheric Environment 41, 1135–1149.

Grell, G.A., Dudhia J., Stauffer, D.R., 1994. A description of the fifth generation Penn State/NCAR mesoscale model (MM5). NCAR Technical Note, NCAR TN-398-STR, 138pp.

Gustin, M.S., et al., 2006. Mercury exchange between the atmosphere and low mercury containing substrates. Applied Geochemistry 21 (11), 1913–1923.

Holmes, C.D., Jacob, D.J., Yang, X., 2006. Global lifetime of elemental mercury against oxidation by atomic bromine in the free troposphere. Geophysical Research Letters 33 (20).

Lin, C.J., Pehkonen, S.O., 1998. Two-phase model of mercury chemistry in the atmosphere. Atmospheric Environment 32 (14–15), 2543–2558.

Lin, C.J., Pehkonen, S.O., 1999. The chemistry of atmospheric mercury: a review. Atmospheric Environment 33 (13), 2067–2079.

Lin, X., Tao, Y., 2003. A numerical modelling study on regional mercury budget for eastern North America. Atmospheric Chemistry and Physics 3, 535–548.

Lin, C.J., Lindberg, S.E., Ho, T.C., Jang, C., 2005. Development of a processor in BEIS3 for estimating vegetative mercury emission in the continental United States. Atmospheric Environment 39 (39), 7529–7540.

Lin, C.-J., et al., 2006a. Trans-Pacific chemical transport of mercury: sensitivity analysis on potential asian emission contribution to mercury deposition in North America using

CMAQ-Hg. In: The 5th CMAS Conference, Research Triangle Park, NC, 16–18 October 2006.

Lin, C.J., et al., 2006b. Scientific uncertainties in atmospheric mercury models I: model science evaluation. Atmospheric Environment 40 (16), 2911–2928.

Lindberg, S.E., Stratton, W.J., 1998. Atmospheric mercury speciation: concentrations and behavior of reactive gaseous mercury in ambient air. Environmental Science & Technology 32 (1), 49–57.

Lindberg, S.E., Meyers, T.P., Taylor, G.E., Turner, R.R., Schroeder, W.H., 1992. Atmosphere-surface exchange of mercury in a forest: results of modeling and gradient approaches. Journal of Geophysical Research 97 (D2), 2519–2528.

Lindberg, S.E., Dong, W.J., Meyers, T., 2002. Transpiration of gaseous elemental mercury through vegetation in a subtropical wetland in Florida. Atmospheric Environment 36 (33), 5207–5219.

Lohman, K., Seigneur, C., Edgerton, E., Jansen, J., 2006. Modeling mercury in power plant plumes. Environmental Science & Technology 40 (12), 3848–3854.

Obrist, D., et al., 2005. Measurements of gaseous elemental mercury fluxes over intact tallgrass prairie monoliths during one full year. Atmospheric Environment 39 (5), 957–965.

Pai, P., Karamchandani, P., Seigneur, C., 1997. Simulation of the regional atmospheric transport and fate of mercury using a comprehensive Eulerian model. Atmospheric Environment 31 (17), 2717–2732.

Pai, P., Karamchandani, P., Seigneur, C., Allan, M.A., 1999. Sensitivity of simulated atmospheric mercury concentrations and deposition to model input parameters. Journal of Geophysical Research-Atmospheres 104 (D11), 13855–13868.

Pai, P., Karamchandani, P., Seigneur, C., 2000. On artificial dilution of point source mercury emissions in a regional atmospheric model. Science of the Total Environment 259 (1–3), 159–168.

Pal, B., Ariya, P.A., 2004a. Gas-phase HO center dot-initiated reactions of elemental mercury: kinetics, product studies, and atmospheric implications. Environmental Science & Technology 38 (21), 5555–5566.

Pal, B., Ariya, P.A., 2004b. Studies of ozone initiated reactions of gaseous mercury: kinetics, product studies, and atmospheric implications. Physical Chemistry Chemical Physics 6 (3), 572–579.

Pan, L., Woo, J.H., Carmichael, G.R., Tang, Y.H., Friedli, H.R., Radke, L.F., 2006. Regional distribution and emissions of mercury in east Asia: a modeling analysis of Asian Pacific Regional Aerosol Characterization Experiment (ACE-Asia) observations. Journal of Geophysical Research 111 (D7).

Pehkonen, S.O., Lin, C.J., 1998. Aqueous photochemistry of mercury with organic acids. Journal of the Air & Waste Management Association 48 (2), 144–150.

Petersen, G., Iverfeldt, A., Munthe, J., 1995. Atmospheric mercury species over central and northern Europe—model-calculations and comparison with observations from the nordic air and precipitation network for 1987 and 1988. Atmospheric Environment 29 (1), 47–67.

Petersen, G., et al., 2001. A comprehensive Eulerian modelling framework for airborne mercury species: model development and applications in Europe. Atmospheric Environment 35 (17), 3063–3074.

Pleim, J.E., Finkelstein, P.L., Clarke, J.F., Ellestad, T.G., 1999. A technique for estimating dry deposition velocities based on similarity with latent heat flux. Atmospheric Environment 33 (14), 2257–2268.

Pongprueksa, P., Lin, C.-J., Ho, T., 2006. Sensitivity evaluation of gas-phase reduction mechanisms of divalent mercury using CMAQ-Hg in a contiguous US domain. In: Extended abstract in the 5th CMAS Annual Conference, Research Triangle Park, 16–18 October 2005.

Ryaboshapko, A., et al., 2002. Comparison of mercury chemistry models. Atmospheric Environment 36 (24), 3881–3898.

Ryaboshapko, A., Artz, R., Bullock, R., Christensen J., Cohen, M., Drexler, R., Ilyin, I., Munthe, J., Pacyna, J., Petersen, G., Syrakov, D., Tranikov O., 2005. Intercomparison study of numerical models for long-range atmospheric transport of mercury. EMEP/MSC-E Technical Report, Leningradsky, 16/2, 125040 Moscow, Russia.

Sanchez-Polo, M., Rivera-Utrilla, J., 2002. Adsorbent-adsorbate interactions in the adsorption of Cd(II) and Hg(II) on ozonized activated carbons. Environmental Science & Technology 36, 3850–3854.

Schmolke, S.R., Petersen, G., 2003. A comprehensive Eulerian modeling framework for airborne mercury species: comparison of model results with data from measurement campaigns in Europe. Atmospheric Environment 37, S51–S62.

Schroeder, W.H., Munthe, J., 1998. Atmospheric mercury—an overview. Atmospheric Environment 32 (5), 809–822.

Seigneur, C., et al., 1998. Mercury adsorption to elemental carbon (soot) particles and atmospheric particulate matter. Atmospheric Environment 32 (14–15), 2649–2657.

Seigneur, C., Karamchandani, P., Lohman, K., Vijayaraghavan, K., Shia, R.L., 2001. Multiscale modeling of the atmospheric fate and transport of mercury. Journal of Geophysical Research—Atmospheres 106 (D21), 27795–27809.

Seigneur, C., Lohman, K., Vijayaraghavan, K., Shia, R.L., 2003a. Contributions of global and regional sources to mercury deposition in New York State. Environmental Pollution 123 (3), 365–373.

Seigneur, C., et al., 2003b. Simulation of the fate and transport of mercury in North America. Journal De Physique Iv 107, 1209–1212.

Seigneur, C., Vijayaraghavan, K., Lohman, K., Karamchandani, P., Scott, C., 2004. Global source attribution for mercury deposition in the United States. Environmental Science & Technology 38 (2), 555–569.

Seigneur, C., Lohman, K., Vijayaraghavan, K., Jansen, J., Levin, L., 2006a. Modeling atmospheric mercury deposition in the vicinity of power plants. Journal of the Air & Waste Management Association 56 (6), 743–751.

Seigneur, C., Vijayaraghavan, K., Lohman, K., 2006b. Atmospheric mercury chemistry: sensitivity of global model simulations to chemical reactions. Journal of Geophysical Research—Atmospheres 111 (D22).

Selin, N.E., Jacob, D.J., Park, R.J., Yantosca, R.M., Strode, S., Jaeglé, L., Jaffe, D., 2007. Chemical cycling and deposition of atmospheric mercury: global constraints from observations. Journal of Geophysical Research—Atmospheres 112 (D2), D02308.

Shia, R.L., Seigneur, C., Pai, P., Ko, M., Sze, N.D., 1999. Global simulation of atmospheric mercury concentrations and deposition fluxes. Journal of Geophysical Research—Atmospheres 104 (D19), 23747–23760.

Walcek, C., De Santis, S., Gentile, T., 2003. Preparation of mercury emissions inventory for eastern North America. Environmental Pollution 123 (3), 375–381.

Wesley, M.L., 1989. Parameterization of surface resistances to gaseous dry deposition in regional-scale numerical models. Atmospheric Environment 23, 1293–1304.

Xu, X.H., Yang, X.S., Miller, D.R., Helble, J.J., Carley, R.J., 1999. Formulation of bi-directional atmosphere-surface exchanges of elemental mercury. Atmospheric Environment 33 (27), 4345–4355.

Xu, X.H., Yang, X.S., Miller, D.R., Helble, J.J., Carley, R.J., 2000a. A regional scale modeling study of atmospheric transport and transformation of mercury. I. Model development and evaluation. Atmospheric Environment, 34 (28), 4933–4944.

Xu, X.H., Yang, X.S., Miller, D.R., Helble, J.J., Carley, R.J., 2000b. A regional scale modeling study of atmospheric transport and transformation of mercury. II. Simulation results for the northeast United States. Atmospheric Environment 34 (28), 4945–4955.